Eliminating Qubit-Type Cross-Talk in the *omg* Protocol

Samuel R. Vizvary,[1,*] Zachary J. Wall,[1] Matthew J. Boguslawski,[1] Michael Bareian,[1]
Andrei Derevianko,[2] Wesley C. Campbell,[1,3,4] and Eric R. Hudson[1,3,4]
[1]*Department of Physics and Astronomy, University of California Los Angeles, Los Angeles, California, USA*
[2]*Department of Physics, University of Nevada, Reno, Nevada 89557, USA*
[3]*Challenge Institute for Quantum Computation, University of California Los Angeles, Los Angeles, California, USA*
[4]*Center for Quantum Science and Engineering, University of California Los Angeles, Los Angeles, California, USA*

(Received 9 November 2023; revised 29 March 2024; accepted 17 May 2024; published 24 June 2024)

The *omg* protocol is a promising paradigm that uses multiple, application-specific, qubit subspaces within the Hilbert space of each single atom during quantum information processing. A key assumption for *omg* operation is that a subspace can be accessed independently without deleterious effects on information stored in other subspaces. We find that intensity noise during laser-based quantum gates in one subspace can cause decoherence in other subspaces, potentially complicating *omg* operation. We show, however, that a magnetic-field-induced vector light shift can be used to eliminate this source of decoherence. As this technique simply requires choosing a specific, magnetic field-dependent polarization for the gate lasers, it is straightforward to implement and potentially helpful for *omg*-based quantum technology.

DOI: 10.1103/PhysRevLett.132.263201

The highest fidelity state-preparation and measurement (SPAM) operations [1] as well as single- and two-qubit gates [2,3] have all been achieved using trapped atomic ions. This performance is realized in part thanks to the high degree of isolation of trapped ion qubits from their environment as compared to other technologies. This isolation necessitates that the *entropic* (or open-channel) operations used to prepare a qubit, i.e. motional cooling and state preparation, are introduced deliberately, typically via laser light that is resonant with atomic electronic transitions. As light from these lasers can be extinguished as needed, they provide a strong but severable link to the environmental bath.

However, if cooling is needed as part of a given quantum operation, due to, e.g., heating during a long algorithm [4] or due to shuttling in the QCCD architecture [5], laser cooling cannot be performed directly since the strong coupling of the process to the atomic internal states scrambles any quantum information hosted in the atom. To overcome this limitation, some ion-based quantum processors simultaneously use two species of atoms [5]. One species, the logic ion, is used to host and process the quantum information, while the other ion, the coolant ion, is used only for cooling.

This "dual species" approach is powerful, providing capabilities like mitigation of heating during transport and long algorithms, as well as facilitating mid-circuit measurement [6]. It is not, however, without complication. Beyond requiring significantly more complicated laser and optical systems, the mass difference of the two species, coupled with the pondermotive nature of an ion trap, leads to deleterious effects such as mode-decoupling [7] and increased heating during transport [8,9]. These necessitate complicated shuttling protocols, specific ion chain arrangements, and significant recooling time after transport [5].

A recent proposal, dubbed the *omg* protocol, has described how to achieve dual-species functionality using a single atomic species [10]. The *omg* protocol leverages the three types of qubits; optical, metastable, and ground, available in certain atomic ions species to host quantum information in different parts of the atomic Hilbert space. Allowing operations to be performed on some ions, while other ions, occupying different parts of the Hilbert space, are protected from the operation. As such, *omg* appears to offer many advantages over the dual-species approach including reducing the number of trapped ions needed for a given algorithm, a reduction in laser and optical complexity, the elimination of the effects associated with mass mismatch, and the ability to flexibly define an ion's role.

However, while some of the basic components of the *omg* protocol have been demonstrated, such as qubit initialization and single-qubit gates [11], many of its promised benefits remain unproven. One open question is the degree to which operations can be performed on one part of the Hilbert space without affecting others. Recent work has shown that in $^{171}Yb^{+}$ both laser cooling and single-qubit Raman gates performed on one manifold cause small but noticeable errors in other storage manifolds [11]. For deep quantum circuits, these operations could lead to significant memory errors within the affected storage subspace, especially when extrapolated to capture the effect of two-qubit cross-talk errors. Here, we show that the high-intensity operations necessary for laser-based gates in the *m*

space of $^{133}Ba^{+}$ do indeed lead to detrimental effects, as the intensity instability of the gate lasers causes uncontrolled differential light shifts for qubits stored in the g manifold. Since the g subspace serves as the storage qubit in the *omg* protocol for $^{133}Ba^{+}$, and using a global gate laser offers significant benefits [10], reducing this error would be highly advantageous. Interestingly, we find this effect can be mitigated by exploiting magnetic-field-induced hyperfine mixing to realize a nonzero, vector light shift between the clock-state qubits that cancels the scalar and tensor shifts [12–16]. Therefore, with the correct laser polarization, which we dub the "magic polarization," the differential light shift of g-type qubits by the gate lasers is nulled, protecting information stored in g-type qubits from m-type qubit laser-based operations.

Implementation of the *omg* protocol in $^{133}Ba^{+}$ utilizes the $\{g, m, g\}$ architecture where the ordered triplet denotes the qubit space used for {cooling, gates, storage} [10]. In this architecture, information is stored in the g subspace and qubits are "activated" to the m subspace for gates, as shown in Fig. 1(a). If the activation resolves single ions, the laser light used for gates can be applied globally, providing a dramatic simplification in system complexity. In this work,

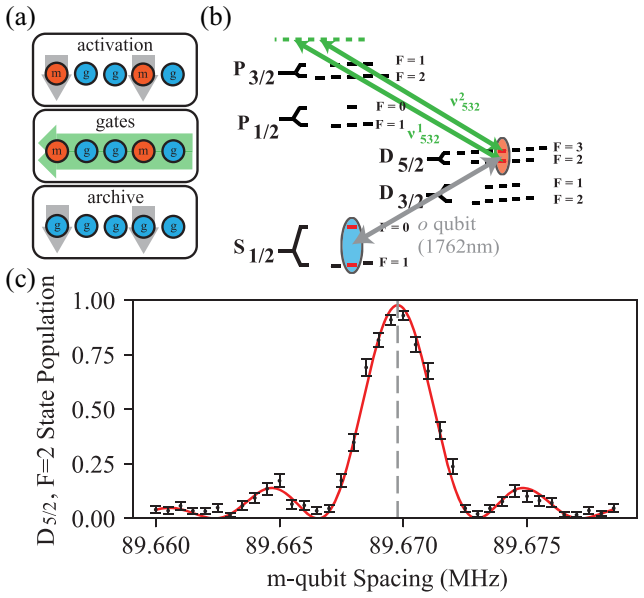

FIG. 1. (a) $\{g, m, g\}$ *omg* protocol for $^{133}Ba^{+}$. Cooling and readout are performed via g qubits in the $^{2}S_{1/2}$ manifold. Activation of the m qubit occurs via the o-qubit transition. Gates are done via global m-qubit beams. Archiving occurs with a transfer back to the g-qubit manifold. (b) Energy level diagram showing both the g (blue) and m (orange) manifolds in $^{133}Ba^{+}$. Both Raman gate beams $(\nu^{1}_{532}, \nu^{2}_{532})$ are split in frequency by the m-qubit spacing and blue detuned from the $P_{3/2}$ resonant transition. (c) Raman spectroscopy of m-qubit hyperfine splitting found to be 89.6697(4) MHz at 5.036(1) G. The power used in each beam is roughly 35 mW and the beam diameter is about 90 μm.

we define the g-type qubit as the $F = 0$ and $F = 1$ hyperfine zero-field clock (i.e. $m_F = 0$) states of the $^{133}Ba^{+}$ $^{2}S_{1/2}$ manifold, while the m-type qubit is defined on the $F = 2$ and $F = 3$ hyperfine zero-field clock states of the $^{2}D_{5/2}$ manifold. Laser cooling, state preparation, and state readout are performed via the g subspace as detailed in Ref. [23]. After high-fidelity state preparation of the $F = 1$, $m_F = 0$ g-qubit state, transfer to the m-type qubit is accomplished via a heralded coherent operation on the o-qubit transition at 1762 nm to the $F = 3$, $m_F = 0$ state of the $^{2}D_{5/2}$ manifold [16]. Readout of the m qubit is performed by a shelving operation that involves the simultaneous application of lasers at 1762 and 493 nm to transfer the target m-state population to the $^{2}D_{3/2}$ manifold, where it can be detected via resonant fluorescence [16]. A continuous wave laser at 532 nm is directed through acousto-optical modulators to generate the beams for stimulated Raman m-type qubit gates. An electro-optical modulator in the beam path allows the same laser to also perform operations on the g-type qubit; while not required by the $\{g, m, g\}$ architecture, the ability to use the same laser path to perform g- and m-qubit gates adds significant flexibility to the system.

Because high-resolution spectroscopy of $^{133}Ba^{+}$ is not yet complete, it is necessary to first measure the hyperfine splitting of the $5d6s\,^{2}D_{5/2}$ state that hosts the m qubit before performing m-qubit gates. We perform this measurement via stimulated Raman spectroscopy on the $F = 3$, $m_F = 0 \leftrightarrow F = 2$, $m_F = 0$ transition at $B = 5.036(1)$ G, as shown in Figs. 1(b) and 1(c). From this measurement, we report the first high-resolution measurement of the $^{133}Ba^{+}$ $5d6s\,^{2}D_{5/2}$ hyperfine constant as $A_{5/2} = 29.7565(1)_{\mathrm{sys}}$ MHz, with a statistical uncertainty of 40 Hz. Using this measurement, we use a single m-qubit rotation to measure the intensity-noise-limited m-qubit coherence time to be 2.6(9) ms [16].

To ascertain the effect of the light used for these m-type gates on a qubit stored in the g subspace, we perform a detuned Ramsey sequence on a g qubit using microwave radiation, with and without illumination by the laser beams used in the m-qubit gate. As seen in Fig. 2(b) for σ^{-} polarization and a magnetic field of $B = 5.00(1)$ G, a fit of the decaying oscillation suggests a g-qubit coherence time of approximately 50 ms. The decay in coherence seen in Fig. 2(b) corresponds to roughly a $2.7(2) \times 10^{-5}$ cross-talk error in the g qubit per m-qubit π pulse. Extrapolating from this error, we estimate a cross-talk error due to a two-qubit gate in the m space of $\gtrsim 10^{-4}$. While these errors are below error correction thresholds [24], it is of course desirable to mitigate them to reduce resource demands.

While this effect could be somewhat mitigated with technical improvements and dynamical decoupling, it would be beneficial if the differential light shift of the g-qubit states could simply be eliminated. To understand

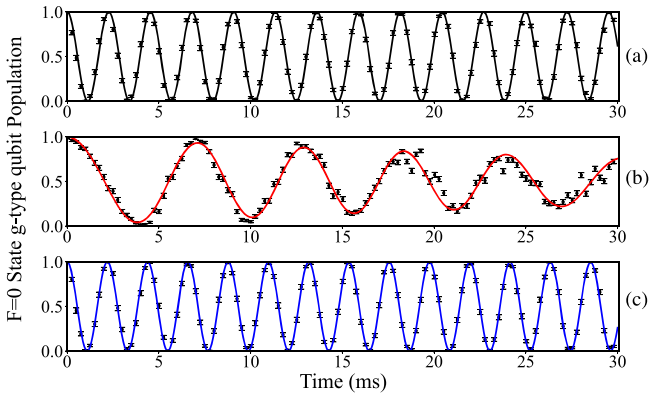

FIG. 2. A detuned microwave Ramsey sequence of the g qubit is performed under different illumination conditions. The frequency of the oscillation corresponds to the detuning of the Ramsey microwave pulse. Population of the g-qubit $F = 0$ state under a detuned microwave Ramsey sequences at 5.00(1) G with (a) no 532 nm gate laser illumination, (b) 532 nm illumination at a nonmagic polarization (σ^-), and (c) 532 nm illumination at the magic polarization.

how this is possible, it is useful to write the light shift of an atomic state due to a laser at frequency ω_L and polarization $\hat{\epsilon}_L$ as $\Delta E_{F,m_F} \propto \alpha_F(m_F, \omega_L, \hat{\epsilon}_L) I_L$, where α_F is the dynamic polarizability and I_L is the laser intensity.

The dynamic polarizability can be decomposed as [25]

$$\alpha_F(m_F, \omega_L, \hat{\epsilon}_L) = \alpha_F^s(\omega_L) + A\frac{m_F}{2F}\alpha_F^a(\omega_L) + \frac{1}{2}(3|\hat{\epsilon}_L \cdot \hat{z}|^2 - 1)\frac{3m_F^2 - F(F+1)}{F(2F-1)}\alpha_F^t(\omega_L), \quad (1)$$

where the m_F-independent α_F^s, α_F^a, and α_F^t are the scalar, vector (axial), and tensor dynamic polarizabilities respectively, $A \equiv -i(\hat{\epsilon}_L^* \times \hat{\epsilon}_L) \cdot \hat{z}$ is the helicity projection of circular polarization and $\hat{z}$ is the quantization axis. At first glance, since the vector and tensor polarizabilities are nonzero only for $F \geq 1/2$ and $F \geq 1$, respectively, and the g-qubit states have $m_F = 0$, it would appear the only opportunity for nulling the differential light shift between the qubit states is via controlling the direction of linear polarization relative to the magnetic field to tune the tensor shift contribution. However, the magnitude of the tensor contribution is not large enough to allow matching the light shift of the two qubit states. Fortunately, in a nonzero magnetic field Eq. (1) is only approximate as the magnetic field breaks rotational invariance and F is no longer a good quantum number. The result is a nonzero vector light shift contribution even for $m_F = 0$ [12–15], which can be used to match the dynamic polarizabilities of the two clock states and null the differential light shift.

This can be intuitively understood by considering the light shift of the g-qubit states under illumination by a laser with σ^+ polarization. The two states couple primarily to the $F = m_F = 1$ state of the $^2P_{1/2}$ manifold [see e.g. Fig. 1(b)]. At zero magnetic field, the $F = 0$ g-qubit state experiences a larger light shift than the $F = 1$ g-qubit state because it is closer to the $^2P_{1/2}$ manifold. Therefore, the g qubit has a negative differential light shift. In a nonzero magnetic field, the two g-qubit states are mixed and the coupling is modified such that the light shift now depends on the degree of helicity projection.

To quantify this effect, we measure the differential light shift of the g qubit using a Ramsey sequence [16] as a function of A and $B\hat{z}$, under the condition that the angle between $\hat{k}$ and $\hat{z}$ is $\theta_{kz} = 180.0(8)°$. As seen in Fig. 3, the g qubit exhibits a clear, magnetic-field dependent vector light shift. Interestingly, above a certain magnetic field this vector light shift is large enough to completely counteract the difference in the scalar light shifts. By using gate lasers operating at a magic polarization where the differential light shift is zero, the g-qubit splitting becomes completely insensitive to the m-qubit gate lasers. The magnetic field required for a given magic polarization is found by finding the zero crossings of the fitted lines in Fig. 3(a), which are plotted as black points in Fig. 3(b). In Fig. 3(b) the error bars are roughly 68% confidence intervals as determined from the fit. The minimum magnetic field necessary for cancellation of the g-qubit light shift, which we call the critical magnetic field B_c, is achieved for $A = 1$ (σ^+ polarization). However, due to coherent population trapping effects [26], our Doppler cooling efficiency suffers below a magnetic field of ~2 G, and therefore we cannot probe the critical magnetic field directly. Instead, we fit the expected theoretical behavior to the data in Fig. 3(b) to extract B_c.

The dependence of the magic polarization on magnetic field is found by diagonalizing the optical Hamiltonian leading to Eq. (1) in the presence of a magnetic field B [28]. The result is a vector light shift term that is proportional to B leading to the relation

$$A \approx -\frac{\hbar\omega_q}{\mu_B B}\sqrt{\frac{2I+1}{2I(2I+2)}}\frac{\alpha_{F'}^s(\omega_L) - \alpha_F^s(\omega_L)}{\alpha_F^a(\omega_L)} \approx \frac{B_c}{B}, \quad (2)$$

where we distinguish between the polarizabilities of the two ($F' = 0$ and $F = 1$) qubit states separated by energy $\hbar\omega_q$. Fitting this expression to the data in Fig. 3(b) yields an experimental value of the critical magnetic field for $^{133}Ba^+$ g qubits of $B_c = 1.15(3)$ G at 532 nm.

Calculation of the expected behavior requires that a third-order hyperfine-interaction (HFI) mediated polarizability treatment [28] be used in Eq. (2) as the two scalar polarizabilities cancel otherwise. This partially stems from the fact that the total electron angular momentum J is

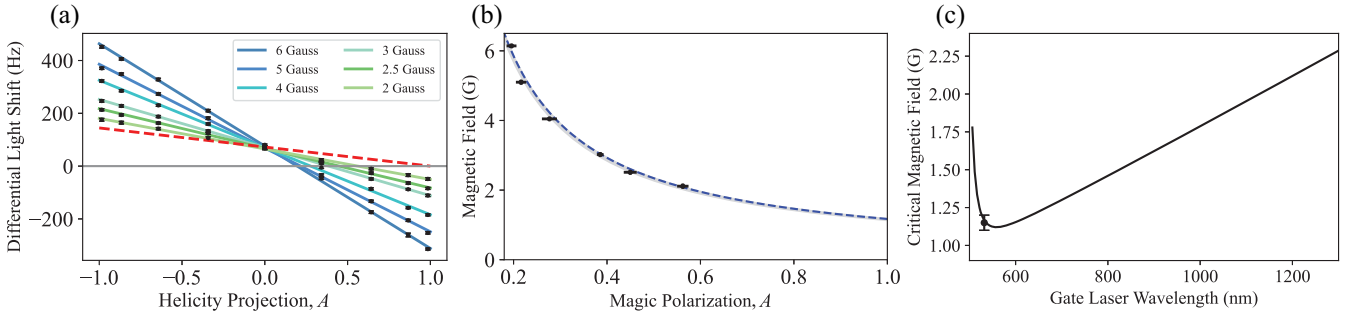

FIG. 3. (a) Differential light shift of g-qubit spacing as a function of the helicity projection, A. The A value corresponding to the zero crossing for each magnetic field is the "magic condition" where the differential shift is zero. The red dashed line represents the theoretical curve for the critical field, B_c, found here. (b) The applied magnetic field versus magic polarization determined from fits of the magic condition in (a). The data are plotted as black dots with error bars given by the fit errors in (a) and the gray shaded area is a 68% confidence interval of the points using an orthogonal distance regression (ODR) fit [27]. The critical field, $B_c = 1.15(3)$ G, is found at $A = 1$ from the fit. The dotted blue line represents an *ab initio* theoretical calculation giving a value of B_c in $^{133}Ba^+$ of 1.17 G at 532 nm. (c) Calculated critical magnetic field as a function of gate laser wavelength. The data point at 532 nm represents the value measured here.

mixed by the atomic hyperfine interaction, leading to differing transition dipole moments for the hyperfine qubit states to the same fine-structure state. Using a combination of empirical data for low-lying electronic states and *ab initio* relativistic RPA + BO many-body method [28–30], we numerically evaluate the polarizabilities in Eq. (2). The results of the numerical calculation are plotted as the dashed blue line in Fig. 3(b), and correspond to a predicted critical magnetic field of $B_c = 1.17$ G at 532 nm, in agreement with the measurement.

The HFI-mediated polarizability calculation has also been performed as a function of gate laser wavelength and the predicted B_c is plotted in Fig. 3(c) alongside the data. The rise in the B_c with large detunings is due to interference from the counter-rotating terms, which work to lessen the induced vector light shift. This difference can be substantial and clearly shows the need for high-level calculations.

To demonstrate the utility of magic polarization for *omg* operation, we repeat the measurements of Fig. 2(b) at $B = 5.00(1)$ G, but with the polarization chosen to be magic ($A = 0.212$). As can be seen in Fig. 2(c), the decoherence due to the light shift of the g qubit by the m-qubit gate laser is mitigated, leading to a ~100-fold increase in coherence time. In fact, the magic g-qubit coherence time of [$\tau = 3.6(2.5)$ s] is consistent with the performance observed when the ion is not illuminated by the gate laser [Fig. 2(a)] despite being exposed to a laser field with an intensity of ~100 MW/m^2. Using the magic polarization, we decrease the g-qubit cross-talk error per m-qubit π pulse from roughly $2.7(2) \times 10^{-5}$ to roughly $3(2) \times 10^{-7}$; a similar 100-fold reduction in cross-talk error for two-qubit gates is expected. As these infidelities are below state-of-the-art single qubit gate infidelities [2], they should not significantly affect use of the *omg* protocol.

For single- and two-qubit gates, $A = 1$ polarization is preferred as it yields the largest Rabi rate and therefore minimizes spontaneous Raman scattering error [17,18]. Thus, to harness the benefits of this magic condition, the applied magnetic field should be at the critical point. However, at 532 nm the critical magnetic field for $^{133}Ba^+$ is well below 2 G, which is the minimum magnetic field we require for efficient Doppler cooling. Luckily, as the gate laser is further detuned to longer wavelengths the critical field grows, due to interference from the emission first term in the light shift, as shown in Fig. 3(c). The use of a longer wavelength gate laser, while requiring moderately more power, has the added benefit of a lower Raman scattering rate. For example, at 1130 nm $B_c \approx 2$ G and the two-qubit gate infidelity due to Raman scattering is expected to be $<10^{-5}$ [18].

In summary, we demonstrate the first preparation, operation, and readout of the m qubit in $^{133}Ba^+$ and report the most accurate measurement to date of the $5d6s\ ^2D_{5/2}$ hyperfine splitting of $A_{5/2} = 29.75650(10)_{sys}(4)_{stat}$ MHz. Using these tools, we examine the cross-talk of global *omg* laser-based gates between qubit subspaces and find that gate operations on m qubits lead to significant decoherence of g qubits. This decoherence results from the g-qubit differential light shift by the gate laser. However, utilizing a magnetic-field-induced vector light shift, we show that the light shift between these zero-field clock-state qubits can be matched using a magic polarization. We measure the critical magnetic field required to realize a magic polarization in $^{133}Ba^+$, compare it to high-level atomic structure calculations, and find good agreement. Finally, using the magic polarization to null the differential light shift of the g-qubit states, we demonstrate protection of quantum information stored in the g qubit from m-qubit laser-based operations.

This work was supported in part by the Army Research Office Grant No. W911NF-20-1-0037 and National Science Foundation Grants No. PHY-2207546 and No. OMA-2016245.

*samvizvary@g.ucla.edu

[1] F. A. An, A. Ransford, A. Schaffer, L. R. Sletten, J. Gaebler, J. Hostetter, and G. Vittorini, Phys. Rev. Lett. **129**, 130501 (2022).
[2] C. J. Ballance, T. P. Harty, N. M. Linke, M. A. Sepiol, and D. M. Lucas, Phys. Rev. Lett. **117**, 060504 (2016).
[3] J. P. Gaebler, T. R. Tan, Y. Lin, Y. Wan, R. Bowler, A. C. Keith, S. Glancy, K. Coakley, E. Knill, D. Leibfried, and D. J. Wineland, Phys. Rev. Lett. **117**, 060505 (2016).
[4] K. Sun, C. Fang, M. Kang, Z. Zhang, P. Zhang, D. N. Beratan, K. R. Brown, and J. Kim, J. Phys. Chem. Lett. **14**, 6071 (2023).
[5] S. A. Moses *et al.*, Phys. Rev. X **13**, 041052 (2023).
[6] J. M. Pino, J. M. Dreiling, C. Figgatt, J. P. Gaebler, S. A. Moses, M. S. Allman, C. H. Baldwin, M. Foss-Feig, D. Hayes, K. Mayer, C. Ryan-Anderson, and B. Neyenhuis, Nature (London) **592**, 209 (2021).
[7] K. Sosnova, A. Carter, and C. Monroe, Phys. Rev. A **103**, 012610 (2021).
[8] G. Shu, G. Vittorini, A. Buikema, C. S. Nichols, C. Volin, D. Stick, and K. R. Brown, Phys. Rev. A **89**, 062308 (2014).
[9] R. B. Blakestad, C. Ospelkaus, A. P. VanDevender, J. M. Amini, J. Britton, D. Leibfried, and D. J. Wineland, Phys. Rev. Lett. **102**, 153002 (2009).
[10] D. T. C. Allcock, W. C. Campbell, J. Chiaverini, I. L. Chuang, E. R. Hudson, I. D. Moore, A. Ransford, C. Roman, J. M. Sage, and D. J. Wineland, Appl. Phys. Lett. **119**, 214002 (2021).
[11] H. X. Yang, J. Y. Ma, Y. K. Wu, Y. Wang, M. M. Cao, W.-X. Guo, Y. Y. Huang, L. Feng, Z. C. Zhou, and L. M. Duan, Nat. Phys. **18**, 1058 (2022).
[12] M. H. Schleier-Smith, I. D. Leroux, and V. Vuletić, Phys. Rev. Lett. **104**, 073604 (2010).
[13] R. Chicireanu, K. D. Nelson, S. Olmschenk, N. Lundblad, A. Derevianko, and J. V. Porto, Phys. Rev. Lett. **106**, 063002 (2011).
[14] H. Kim, H. S. Han, and D. Cho, Phys. Rev. Lett. **111**, 243004 (2013).
[15] J. M. Choi and D. Cho, J. Phys. Conf. Ser. **80**, 012037 (2007).
[16] See Supplemental Material at http://link.aps.org/supplemental/10.1103/PhysRevLett.132.263201, which includes Refs. [17–22], for additional information about the experimental methods and a detailed discussion of the magnetic-field-induced hyperfine mixing.
[17] I. D. Moore, W. C. Campbell, E. R. Hudson, M. J. Boguslawski, D. J. Wineland, and D. T. C. Allcock, Phys. Rev. A **107**, 032413 (2023).
[18] M. J. Boguslawski, Z. J. Wall, S. R. Vizvary, I. D. Moore, M. Bareian, D. T. C. Allcock, D. J. Wineland, E. R. Hudson, and W. C. Campbell, Phys. Rev. Lett. **131**, 063001 (2023).
[19] P. Rosenbusch, S. Ghezali, V. A. Dzuba, V. V. Flambaum, K. Beloy, and A. Derevianko, Phys. Rev. A **79**, 013404 (2009).
[20] Q.-Q. Hu, C. Freier, Y. Sun, B. Leykauf, V. Schkolnik, J. Yang, M. Krutzik, and A. Peters, Phys. Rev. A **97**, 013424 (2018).
[21] V. A. Dzuba, V. V. Flambaum, K. Beloy, and A. Derevianko, Phys. Rev. A **82**, 062513 (2010).
[22] S. L. Woods, S. R. Lundeen, and E. L. Snow, Phys. Rev. A **80**, 042516 (2009).
[23] J. E. Christensen, D. Hucul, W. C. Campbell, and E. R. Hudson, npj Quantum Inf. **6**, 35 (2020).
[24] E. Knill, Nature (London) **434**, 39 (2005).
[25] L. R. N. L. Manakov and V. D. Ovsiannikov, Phys. Rep. **141**, 320 (1986).
[26] H. R. Gray, R. M. Whitley, and C. R. Stroud, Opt. Lett. **3**, 218 (1978).
[27] P. T. Boggs, R. H. Byrd, J. E. Rogers, and R. B. Schnabel, User's reference guide for ODRPACK version 2.01: Software for weighted orthogonal distance regression (1992), https://api.semanticscholar.org/CorpusID:126352852.
[28] A. Derevianko, Phys. Rev. A **81**, 051606(R) (2010).
[29] H. B. Tran Tan and A. Derevianko, Phys. Rev. A **107**, 042809 (2023).
[30] D. Xiao, H. B. Tran Tan, and A. Derevianko, Phys. Rev. A **108**, 032805 (2023).